Saturation of Photodiode at High Intensity

Lim Zheng Jie Janet
A0102464R

Supervised by:
Professor Christian Kurtsiefer

A Report Submitted for the Fulfilment of
Undergraduate Research Opportunities in Science

Department of Physics
National University of Singapore

Acknowledgements

I would to thank my supervisor Professor Christian Kurtsiefer for giving me the opportunity to work with the group. Your encouragements motivated me to work even harder. My short stint with the group was definitely an adventurous and enjoyable one.

Very special thanks to Victor and Yi Cheng for their meticulous guidance and patience throughout the project. This report would not have been successfully completed without the help from you guys.

I would also like to thank Wilson for imparting his knowledge and prompting me to strive for the better.

Last but not least, to everyone in the group, thank you for making my special semester an extra special one. (:

Contents

Abstract

In this report, we study the optical response of the Hamamatsu S5107 Silicon PIN Photodiode at high optical intensity. An optical circuit was set up with a 780nm laser diode. The beam waist of the Gaussian laser beam was obtained through the Knife-edge measurements, and found to be 0.0091mm. Saturation can be observed above a threshold intensity of $0.04\text{W}(\text{mm})^{-2}$.

1   Introduction

The silicon photodiode is a semiconductor device responsive to high energy photons, and is commonly used as a light sensor. They feature high-speed response, high sensitivity and low noise. Silicon photodiodes are widely utilized in applications such as spectroscopy and optical communications.[1]

Photodiodes operate by absorption of photons or charged particles, and produce charge carriers that generate a flow of current in an external circuit. The photodiode reponse is linear if the generated photocurrent increases linearly with the incident light power. If the incident optical intensity is sufficiently high, the photodiode is saturated and non-linearity sets in; a further increase in optical power no longer causes a linear increase in photocurrent. Thus, there is a need to study this non-linearity in order to utilise the photodiode correctly at high intensities.

1.1   Photodiode

The Hamamatsu S5107 silicon PIN photodiode is used throughout this work.

1.1.1   P-N junction

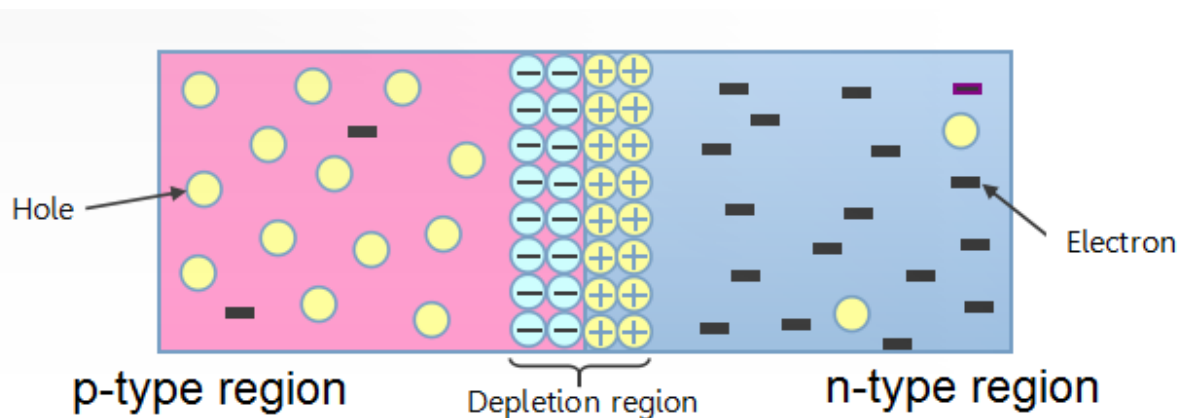Figure 1 illustrates the principle of a p-n junction.

Figure 1: P-N junction[2]

A photodiode is made up of an active p-n junction that operates in a reverse biased state. A p-n junction is formed by joining n-type and p-type semiconductor materials. The n-type

region has a high electron concentration and the p-type region has a high hole concentration. When both regions are in contact, electrons diffuse from the n-type region to the p-type region, and holes diffuse from the p-type region to the n-type region. Movement of electrons to the p-type region exposes positive ion cores in the n-type region, while movement of holes to the n-type region exposes negative ion cores in the p-type region, resulting in an electric field at the junction. The electric field quickly sweeps free carriers out, hence the region is depleted of free carriers. This region is known as the depletion region. A built-in voltage is simultaneously created across the depletion region with the positive potentials at the n-type region and negative potential at the p-type region.

1.1.2 Silicon PIN Photodiode

The most common photodiode detector is the Silicon PIN photodiode. The Silicon PIN photodiode is capable of delivering high-speed response when operated with an applied reverse voltage. In this device, there is a region of undoped intrinsic semiconductor material between the p-type and n-type region[3]. This is shown schematically in Figure 2.
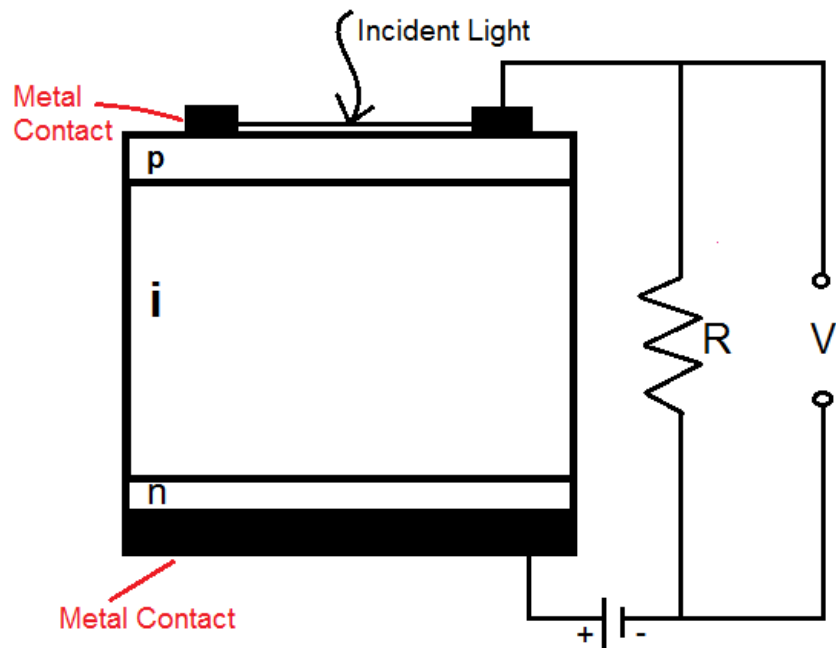
Figure 2: Cross section of the silicon PIN photodiode, showing the intrinsic region between the p-type and n-type regions. The PIN photodiode is operating in the photoconductive mode where a reverse bias is applied.

This intrinsic region serves to increase the width of the junction by having a huge amount of charge carriers from the p-type and n-type regions[4]. This in turn provides for more efficient conversion of photons to charge carriers and increased responsivity.

1.1.3 Charge Carrier Generation

When photons of energy greater than the bandgap of silicon (approximately 1.1 eV)[5] are illuminated onto the photodiode, they are absorbed and electron-hole pairs, which are charge carriers, are created. PIN photodiodes are designed in such a way that fewer charge carriers are generated outside the depletion layer[3].

The separated electron and hole are then attracted by the positive and negative terminals respectively. If the two sides are electrically connected, a generated external current will flow through the connection, and this current is known as the photocurrent. However, if the created charge carriers of that region recombine with the bulk carriers of the same region before reaching the junction field, the carriers are lost and no external current flows[6].

1.1.4 Reverse Bias

In the reverse-biased state, a voltage is applied across the device such that it adds to the built-in voltage and enhances the flow of charge carriers, resulting in a wider depletion region. The higher electric field in the depletion region decreases the probability that charge carriers can diffuse from one side of the junction to the other, hence the diffusion current decreases[7].

1.1.5 Photocurrent

The amount of photocurrent (I_p) generated is dependent on the amount of incident optical power (P)[8]. It follows that as more photons are incident on the active area of a photodiode, more charge carriers will be created, and thus a higher photocurrent generated. This relationship is represented by Equation 1.

$$I_p = sP \tag{1}$$

where,
s = Responsivity of the photodiode.

1.1.6 Saturation Effect

However, at high intensity, it is expected that the incident light power and generated pho-
tocurrent do not exhibit a linear relationship[4], and the photodiode is saturated. This is
possibly due to the depletion of available electron-hole pairs, thus excess photons will not be
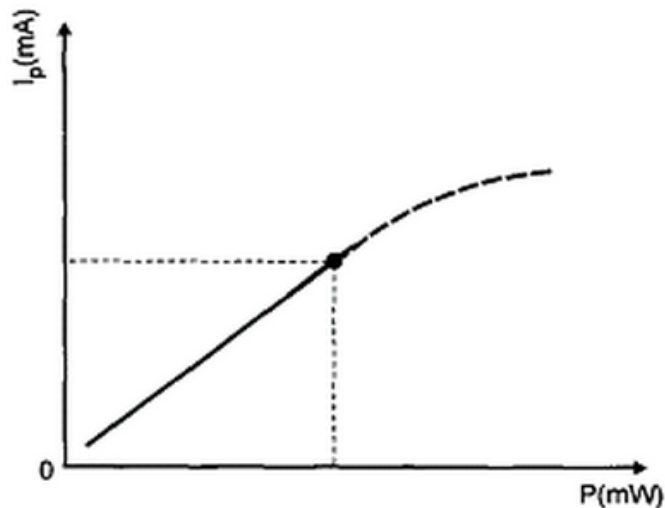absorbed. This phenomenon can be illustrated by Figure 3.

Figure 3: Relationship between incident optical power and generated photocurrent[4]

1.2 Light Source

The laser diode used in this experiment is of a wavelength of 780nm. The output of the
laser diode is subsequently modified by experimental means to a Gaussian beam, as will be
elaborated in Section 2.1.

1.2.1 Gaussian beam

The Gaussian beam is a beam of electromagnetic radiation whose transverse electric field
and intensity distributions are well approximated by Gaussian functions[9]. The intensity
distribution of a Gaussian beam is,

$$I(r, z) = \frac{2P}{\pi w^2(z)} \exp(\frac{-2r^2}{w^2(z)}) \tag{2}$$

4

where,

P = Input power

r = Radial coordinate

$w(z)$ = Beam radius at any position z

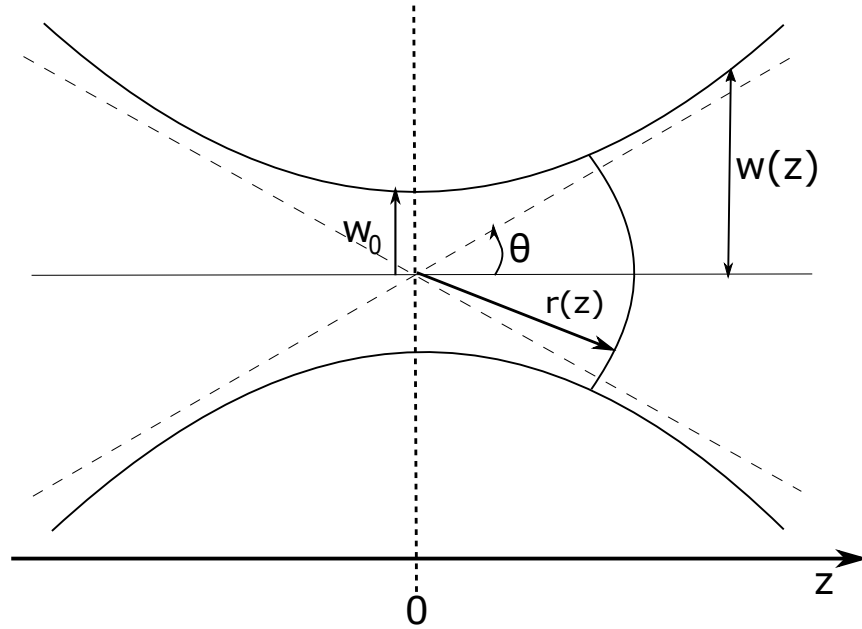The geometry of a Gaussian beam is governed by a set of beam parameters as shown in Figure 4.

Figure 4: The Gaussian profile

For a propagating Gaussian beam, $w(z)$ will be at a minimum value w_0, known as the beam waist, at one point along the optical axis. For a beam of wavelength λ at a distance z along the beam from the beam waist, the variation of the spot size is given by,

$$w(z) = w_0 \sqrt{1 + (\frac{z}{z_R})^2} \tag{3}$$

where the origin of the z-axis is defined to coincide with the beam waist, and the Rayleigh range z_R is given by,

$$z_R = \frac{\pi w_0^2}{\lambda} \tag{4}$$

2 Methodology

In order to study the optical response of the photodiode, the measurements of the beam profile and corresponding power of photocurrent are required to allow for analysis.

2.1 Experimental Setup

The experiment is set up as shown in Figure 5. 780nm Light is emitted from a GaAs semiconductor laser diode (EYP-RWE-0790). The typical lasing wavelength of the laser diode used in this experiment is 780nm. The light is coupled to a single mode fiber (Thorlabs 780HP), with an aspheric lens (Thorlabs C220). The fibre output is collimated by another aspheric lens (Thorlabs C220) and focused by a lens ($f = 50$mm) onto a photodiode that is mounted on a calibrated translation stage. A knife edge is mounted on another calibrated translation stage between the lens and the photodiode, and is used to measure the beam profile.
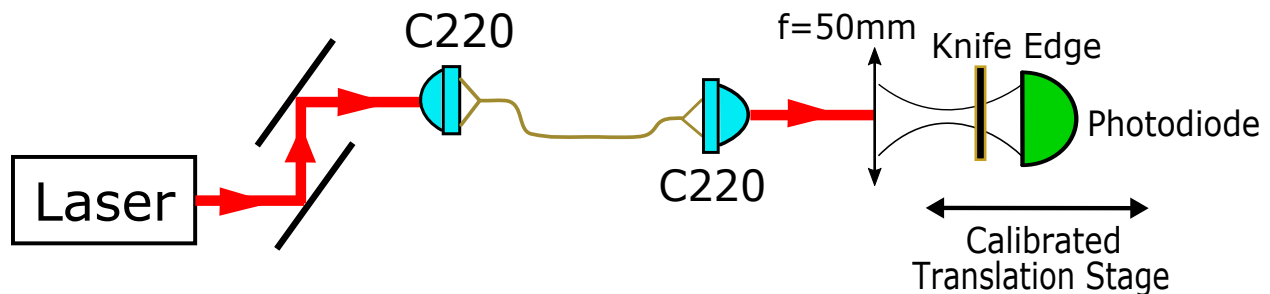

Figure 5: Schematic of the experimental set up

2.2 Beam Waist Measurement

A Gaussian beam is defined by the size and position of the beam waist (w_0) and the wavelength (λ). Therefore, just by determining the size and position of the beam waist, it is possible to fully characterize a Gaussian beam. This can be done by making a series of knife-edge measurements[10] to determine the beam size w(z) as a function of the position z; $w(z)$.
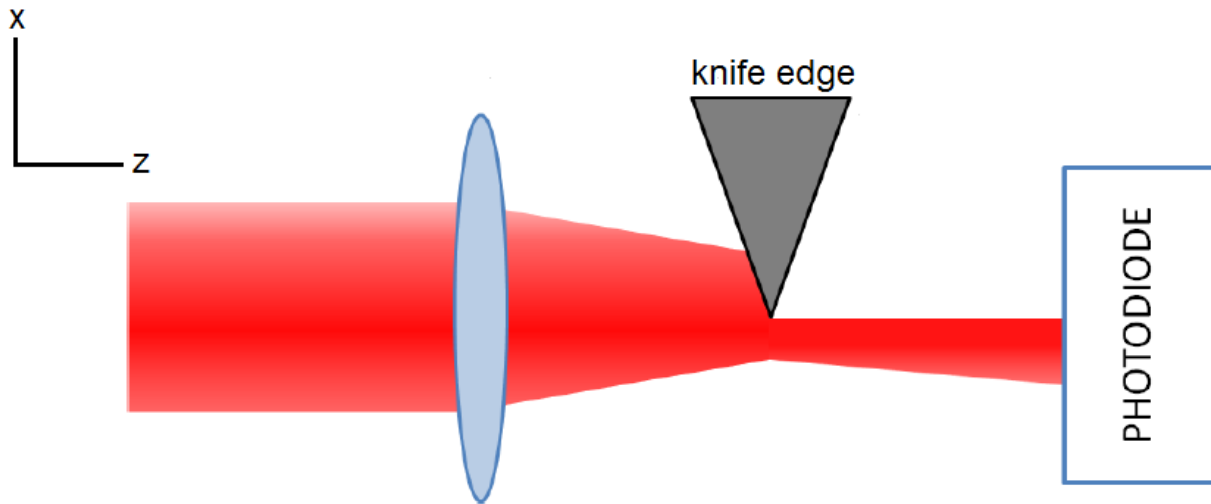
Figure 6: Schematic of the knife edge Measurement[11]

Figure 7 shows the schematic diagram of the knife-edge measurement.

A translation stage moving along z sets the position of the knife edge along the focused beam. The knife edge is initially positioned along x such that it does not interfere the beam. The translation stage is then mounted onto a motor that moves the knife edge in the x direction. As the knife edge progressively covers portions of the beam, the photodiode measures a decrease in optical power. Figure 7 shows a typical measurement curve obtained by a single knife edge measurement.
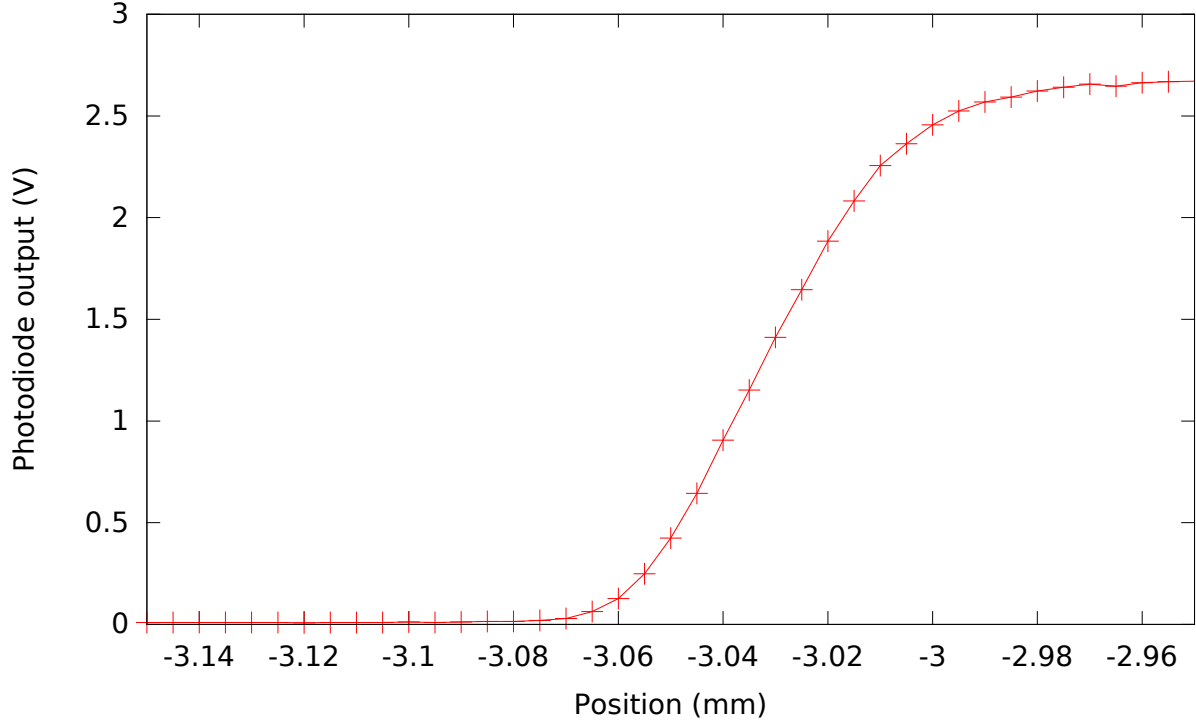
Figure 7: For beam not covered by the knife edge, the measured power reaches its maximal value. On the other hand, the measured power is minimal when the knife edge covers the whole laser beam.

By fitting the data to Equation 5, we obtain the beam size $w(z)$.

$$P = P_0 + \frac{P_{max}}{2}(1 - \text{erf}(\frac{\sqrt{2}(x - x_0)}{w}))$$ (5)

where,

P_0 = Background noise floor

P_{max} = Total power of the beam

x_0 = Position of shift

erf = Standard error function.

The process is then repeated for different position z.

2.3 Power Measurement

To ensure saturation of the photodiode, the laser diode is driven at a high current (approximately 150mA), so as to obtain a sufficiently large optical power. With the photodiode mounted onto a calibrated translation stage, the photodiode is traversed over the distance z, as illustrated in Figure 8 below.
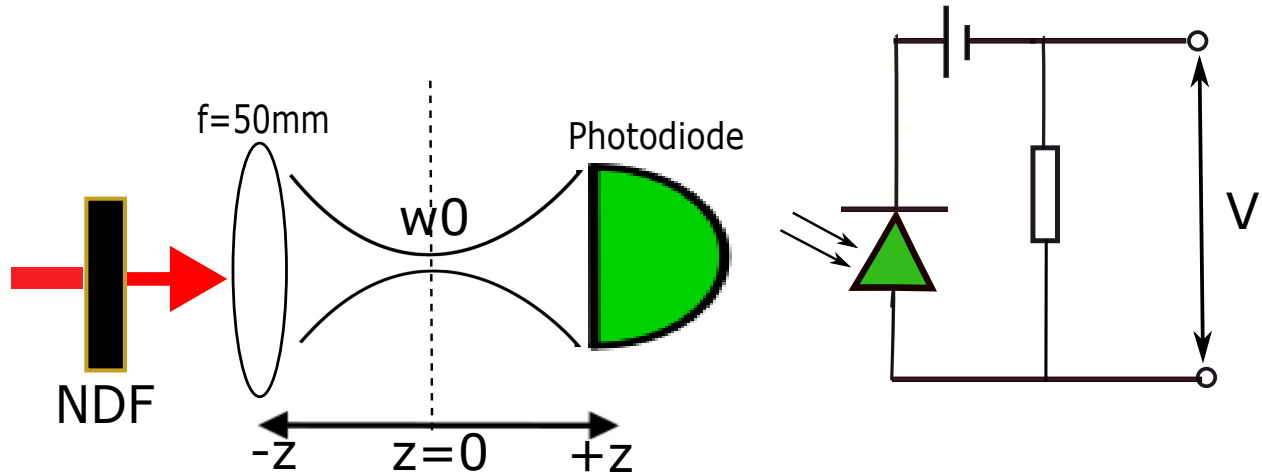

Figure 8: Photodiode is traversed over the variable distance z (varied beam size), from the position of the beam waist, where the output is measured by connecting the photodiode to a multimeter. A Neutral Density Filter (NDF)is added before the lens to vary the input power by factor of OD.

The photocurrent is measured by sending the output of the photodiode through a resistor and measuring the potential difference (V) across it. The power can be calculated using Equation 1. By placing a specified Neutral Density Filter (NDF) in front of the lens, we can vary the optical power incident on the photodiode, such that we can observe different saturation levels for different input powers.

3 Results and Discussion

The measurements are done with a constant input beam of λ=780nm, with beam size of w_i = 0.137mm, power of P_0 = 13.5mW. A resistor of R=100Ω is used in the external circuit of the photodiode, with a reverse-biased voltage of 9V. The Hamamatsu S5107 silicon PIN photodiode, with a responsivity of $s = 0.59\text{AW}^{-1}$[12] is used throughout this work.

3.1 Beam Waist Measurement

The beam size measurements are shown in Figure 9. Fitting the data to Equation 3, the beam waist and Rayleigh range was found to be,

$$w_0 = 0.0091 \pm 0.0001\text{mm}$$

$$z_R = 0.3359 \pm 0.0001\text{mm}$$

The fitted Gaussian beam profile is also plotted as shown in Figure 9.
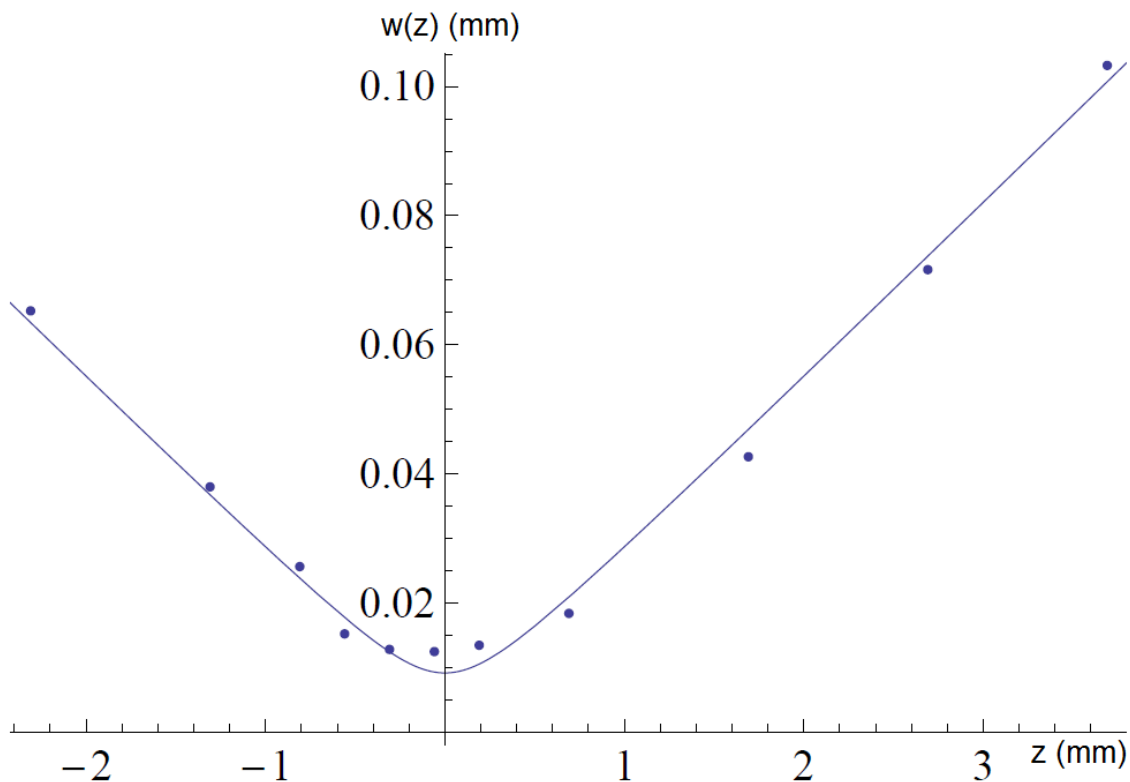

Figure 9: Beam size measurements and fitted beam waist profile

3.1.1 Analysis

The percentage error of this fitted value is approximately 1%. However, even though the error on this fit is relatively small, the measured values deviate from the fitted profile near $z = 0$ (refer to Figure 9). Coupled with the fact that the error bars on each measurements are very small, it suggests that the measured beam profile does not follow a Gaussian beam profile to some extent.

3.2 Power Measurement

The photocurrent from the photodiode is measured by sending it through a resistor (of known value) and measuring the potential difference across the resistor with a multimeter as shown in Figure 8. The output power is represented by,

$$P = \frac{i}{s} = \frac{V/R}{s} \tag{6}$$

Where,
$P = $ Output power
$s = $ Responsivity of photodiode

At high incident light intensity, photocurrent varies non-linearly with the intensity. This can be modelled by,

$$j(r) = \alpha I(r) - \beta I(r)^2 \tag{7}$$

where,
j$(r) = $ Current density
I$(r) = $ Optical intensity

We obtain the current i by integrating j(r) over the whole photodiode.

$$i = \int j dA \approx \int_0^{2\pi} \int_0^\infty j(r) \cdot r dr d\theta \tag{8}$$

where the approximation is justified since the photodiode is much larger than the beam size.

Since the intensity of Gaussian beam is,

$$I(r,z) = \frac{2P}{\pi w^2(z)} exp(\frac{-2r^2}{w^2(z)})$$

From Equations 2,7,8, will allow us to derive an expression of V in terms of z, given by,

$$V(z) = PR\alpha - \frac{P^2 R}{\pi w(z)^2}\beta \tag{9}$$

Using Equation 3, we get,

$$V(z) = PR\alpha - \frac{P^2 R}{\pi w_0^2 + (\frac{\lambda^2}{\pi w_0^2})z^2}\beta = A - \frac{B}{K + K'z^2} \tag{10}$$

with,

$$A = PR\alpha \tag{11}$$

$$B = P^2 R\beta \tag{12}$$

$$K = \pi w_0^2 \tag{13}$$

$$K' = \frac{\lambda^2}{\pi w_0^2} \tag{14}$$

We fit the data to the above mentioned model. Using A and B as free parameters, with $\lambda = 780$ nm, and w_0=0.0091 mm from our measurement in Section 3.1,

$$A = 0.761 \pm 0.003V \rightarrow \alpha \approx 0.566 \pm 0.002 \text{AW}^{-1}$$

$$B = (0.042 \pm 0.005) \times 10^{-3}V \rightarrow \beta \approx (2.3 \pm 0.3) \times 10^{-3}\text{AW}^{-2}(\text{mm})^2$$

If we use w_0 as a free parameter (C) in addition to A and B, the fit then yields,

$$A = 0.790 \pm 0.001V \rightarrow \alpha \approx 0.5872 \pm 0.0007 \text{AW}^{-1}$$

$$B = (0.36 \pm 0.01) \times 10^{-3}V \rightarrow \beta \approx (19.6 \pm 0.6) \times 10^{-3}\text{AW}^{-2}(\text{mm})^2$$

$$C = 0.0299 \pm 0.0004\text{mm} \rightarrow w_0 \approx 0.0299 \pm 0.0004\text{mm}$$

The uncertainties above are determined with the assumption that the errors for P and R are negligible.

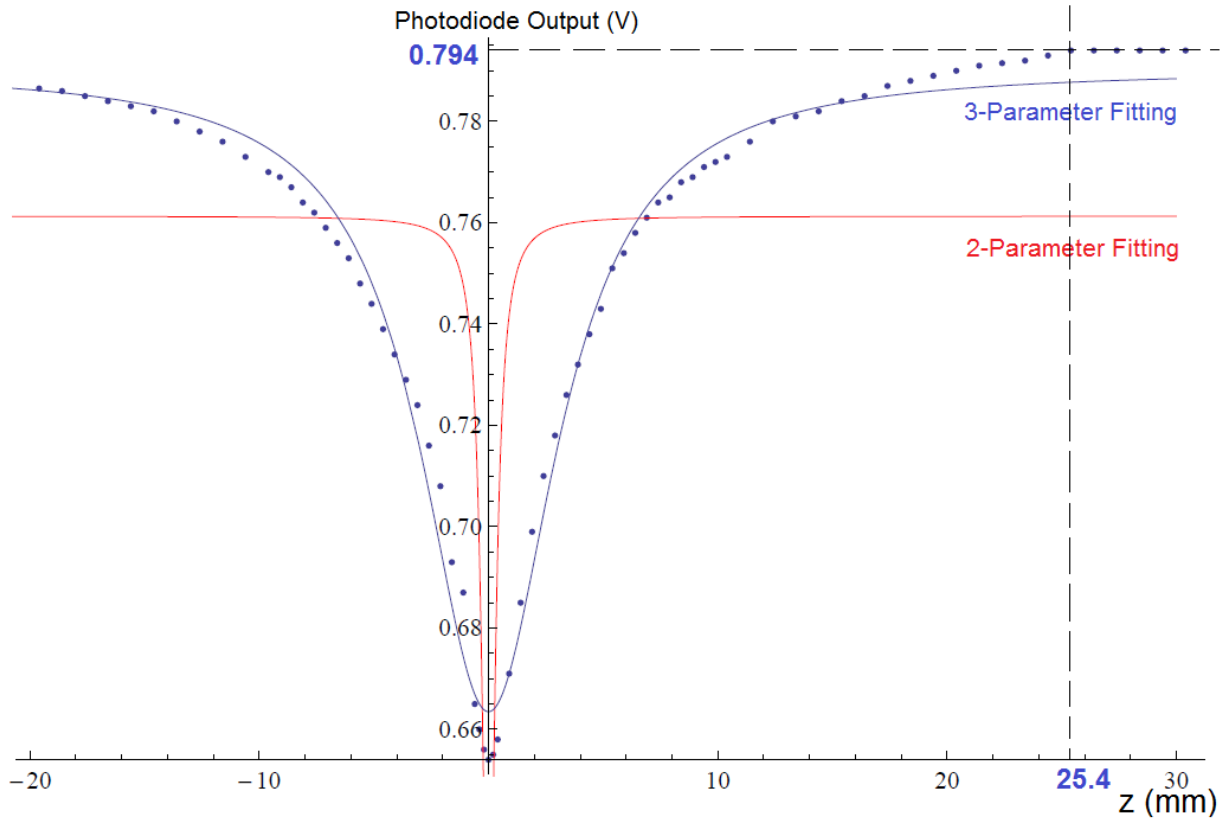The results of the fit are plotted as shown in Figure 10.

Figure 10: Photodiode output at different photodiode positions, using a resistor of R=100Ω. The solid lines shows the results of the fit.

The experiment was repeated with different input optical powers by placing known values of Neutral Density Filters (NDF) before the lens, as mentioned in Section 3.2.

The results are shown in Figure 11, where each curve is normalised to its respective value at z =10mm.
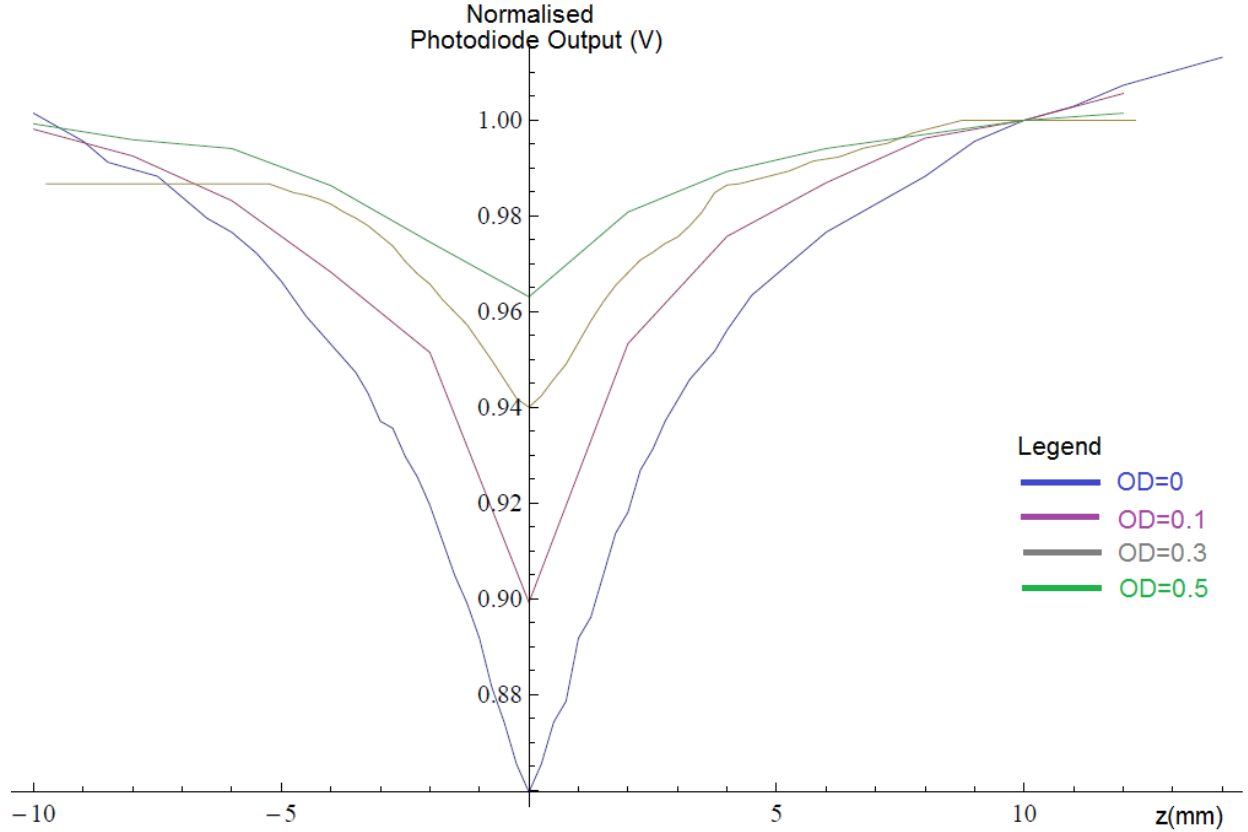
Figure 11: A comparison of the normalised power measurements at different photodiode positions, performed with Neutral Density Filters, and a resistor of R=1000Ω.

3.2.1   Analysis

Comparing the two fits

Figure 10 shows that we will get a better fit by using w_0 as a free parameter.

Using w_0 as a free parameter in the model yields $w_0 \approx 0.0299 \pm 0.0004$mm while the beam waist measurement in section 3.1 yields $w_0 \approx 0.0091 \pm 0.0001$mm. These two values have a percentage difference of approximately 69%.

One can think of three possibilities to explain this discrepancy.

1. In Section 3.1.1 , we mentioned that the beam size measurements deviate from the fitted profile near $z = 0$. It is probably because that the beam is not Gaussian, that the

14

model fails since it assumes a Gaussian beam.

2. The suggested model does not fully reflect the physical phenomena in a saturated photodiode. A better model may involve higher-order or non-polynomial terms.

3. Experimental errors that might include:

    a. The knife edge is uneven and may be slanted during the course of the waistscan. Both of which leads to inaccuracy of beam measurement.

    b. Calibration error of the devices used, such as the motor driver which moves the knife edge.

    c. The beam is not shone on the same spot on the photodiode with each successive illumination. The photodiode might have been shifted slightly from its original position if the micrometer is not adjusted with care. Both of which leads to inaccuracy of power measurement.

However, each measurement of the waistscan gives a good fit with very low errors, thus it is highly unlikely for the beam waist measurement to be flawed by a factor of 3. Therefore the most probable reason should be due to the postulation of a wrong model.

Physical meaning of α and β

In our model, α represents the responsivity of the photodiode. At low input optical power, $\alpha\ I(r) >> \beta\ I^2(r)$, hence yielding a linear relationship between the output current and optical intensity. In addition, the fitted value of $\alpha = 0.587 AW^{-1}$ matches closely to the datasheet value of $\alpha = 0.59 AW^{-1}$ for the photodiode used throughout the experiment.

Judging from the fitted value of $\beta = 1.9613 \times 10^{-4}\ AW^{-1}(\text{mm})^2$, we can infer that β might be a factor associated with the charge carrier creation at saturation. It could be possible that β represents the extent of the number of charge carriers generated.

Comparing results of different NDF

In Figure 11, we can see that as the attenuation of the input optical power increases, the dip of the normalised curve gradually diminishes. This is consistent with our suggested model

in Equation 7 , where we expect a larger saturation (a lager dip) at higher values of $I(r)^2$.

The results also mean that there is a specific maximum intensity that this photodiode can function without saturating. In Equation 2, intensity of a Gaussian beam is defined to be,

$$I(r,z) = \frac{2P}{\pi w^2(z)} Exp(\frac{-2r^2}{w^2(z)})$$

We define the threshold saturation intensity as the intensity at the centre (r=0) of the Gaussian beam of which saturation starts to occur. Using data from Figure 10, saturation is observed when $z = 25.4$mm, with V = 0.794V, R = 100Ω, s = 0.59AW^{-1} (from datasheet). Therefore the threshold intensity below which the photodiode can function without saturation is,

$$I \approx 0.04\text{W(mm)}^{-2}$$

4   Conclusions

A focused Gaussian beam was successfully characterised. The photodiode ouput was measured at different beam sizes and intensities. Saturation of the photodiode was observed above a threshold intensity of 0.04 W(mm)$^{-2}$.

References

[1] "Photodiode charateristics and applications." [Online]. Available: http://www.osioptoelectronics.com/application-notes/AN-Photodiode-Parameters-Characteristics.pdf

[2] "The measurement of a transverse profile of laser beam by knife edge method," 2014. [Online]. Available: http://conceptselectronics.com/diodes/structure-pn-junction-diode/

[3] Wikipedia, "Pin diode."

[4] "Photodiodes," 2013. [Online]. Available: http://www.ni.com/white-paper/14839/en/

[5] "Semiconductor band gaps." [Online]. Available: http://hyperphysics.phy-astr.gsu.edu/hbase/tables/semgap.html

[6] "Pn junction theory." [Online]. Available: http://www.electronics-tutorials.ws/diode/diode_2.html

[7] "Formation of a pn-junction." [Online]. Available: http://www.pveducation.org/pvcdrom/pn-junction/formation-pn-junction

[8] "Photodiode light detector." [Online]. Available: http://hyperphysics.phy-astr.gsu.edu/hbase/electronic/photdet.html

[9] R. Photonics, "Gaussian beam."

[10] J. Q. C. Durham University, "Gaussian beams."

[11] "The measurement of a transverse profile of laser beam by knife edge method," 2014. [Online]. Available: http://people.fjfi.cvut.cz/blazejos/public/ul7en.pdf

[12] Hamamatsu, "Si pin photodiode s5107 datasheet."